

## Effect of Ag Nanoparticles for Electrochemical Sensing of Brilliant Cresyl Blue

Mao-Guo Li,<sup>†,††</sup> Ying-Chun Gao,<sup>†</sup> Xian-Wen Kan,<sup>†,††</sup> Guang-Feng Wang,<sup>†</sup> and Bin Fang<sup>\*,†,††</sup>

<sup>†</sup>School of Chemical and Material Sciences, Anhui Normal University, Wuhu, 241000, P. R. China

<sup>††</sup>Anhui Key Laboratory of Functional Molecular Solids, Anhui Normal University, Wuhu, 241000, P. R. China

(Received November 30, 2004; CL-041457)

The modification of gold electrode by 1,4-benzenedimethanethiol (BDT) self-assembled monolayer and Ag nanoparticles was prepared and its electrochemical sensing of brilliant cresyl blue (BCB) was observed. The results suggested that the methods of electrochemical determination on the modified electrode could be applied in many fields.

In recent years, the study of nanoparticles of noble metals has been an extremely active area because of their interesting properties that are different from those of bulk substances.<sup>1–3</sup> Intriguing prospects for the development of novel electronic device, electro-optical applications, catalysis, sensor technology, and biomolecular labeling<sup>4,5</sup> have been suggested because of their size-dependent properties and quantum size effect.<sup>6,7</sup> Many papers about the metal nanoparticles modified electrode were published.<sup>8–10</sup> However, as we are known, silver is a good conductor of electricity, and the silver ion can easily combine with many compounds in human body by electrovalent bond or coordinate bond.<sup>11,12</sup> In this letter, the self-assembled monolayer electrode was prepared and electrochemical behaviors of brilliant cresyl blue (BCB) as an electrochemical probe were reported. It was observed that the modified electrode could catalyze the redox process of BCB.

The silver nanoparticles were prepared according to the literature<sup>13</sup> and were characterized by UV-vis spectroscopy<sup>14</sup> and transmission electron microscopy. As can be seen from Figure 1, calculation showed that the mean diameter ( $D$ ) of the small silver particles was 21.6 nm and that the standard deviation ( $\sigma$ ) was 2.64%, which were derived from an average of 200 particles. The polydispersity defined as the ratio  $\sigma/D$  was 0.122.

The pretreated gold electrode ( $\Phi = 1.5$  mm) was electrochemically cleaned by cycling the potential scan between  $-0.2$  and  $1.5$  V in freshly deoxygenated  $0.5$  mol/L  $H_2SO_4$  solution until the CV characteristic of clean polycrystalline gold electrode was established. The cleaned electrode was thoroughly rinsed with water and absolute ethanol and it was immersed in BDT solution for 48 h at room temperature in darkness. The re-

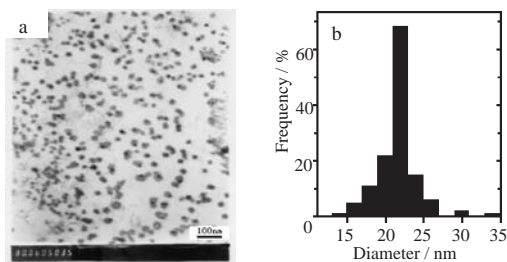


**Figure 1.** (a) TEM and (b) particle size distribution of Ag nanoparticles.

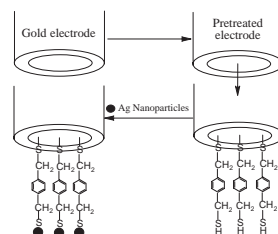


**Figure 2.** The scheme of preparing the modified electrode.

sulting self-assembled electrode was rinsed thoroughly with twice-distilled water and soaked in water for 18 h to remove the physically adsorbed BDT. Then, it was dipped into the colloidal silver for 24 h at  $4$  °C. In such a way, a BDT self-assembled monolayer and Ag nanoparticle-modified gold electrode was prepared. The preparation process of the electrode was shown in Figure 2. All resulting electrodes were washed with water and stored in the pH 7.0 phosphate buffer solution (PBS) at  $4$  °C for use.

The impedance measurement was performed to observe the adsorption process of BDT and Ag nanoparticles.

Figure 3a showed EIS of the bare gold electrode. There was almost a very small semicircle domain as was reported in literature,<sup>15</sup> implying very low electron transfer resistance to the redox-probe dissolved in the electrolyte solution. The EIS of the BDT self-assembled monolayer (Figure 3b) showed a little higher interfacial electron transfer resistance indicating that the BDT monolayer obstructed electron transfer of the electrochemical probe. Figure 3c was the typical Nyquist plots ( $-Z''$  vs  $Z'$ ) for the adsorption process of Ag colloid on BDT modified gold electrode. It showed that the EIS of silver colloid-BDT gold electrode was higher to that of BDT modified gold electrode. This implied that the conductivity of the silver colloid-BDT gold electrode was higher than a bare gold electrode. The reason may be that there was negative charge on the surface of the silver colloids, which would limit the access of ferri/ferrocyanide to

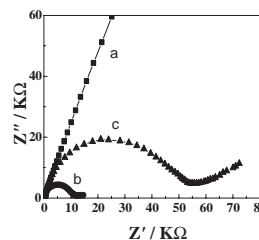


**Figure 3.** The Nyquist plots for different electrodes recorded in  $2.5 \times 10^{-3}$  mol/L  $K_3[Fe(CN)_6]/K_4[Fe(CN)_6]$ : (a) bare gold electrode; (b) BDT self-assembled monolayer gold electrode; (c) BDT self-assembled monolayer and Ag nanoparticle-modified gold electrode.

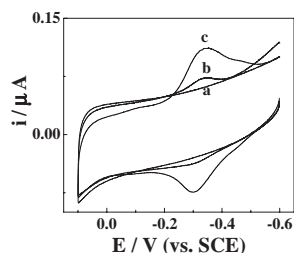


**Figure 4.** Cyclic voltammograms of different electrodes in pH 7.0 PBS containing  $1.0 \times 10^{-5}$  mol/L BCB solution: (a) BDT modified gold electrode; (b) bare gold electrode; (c) BDT and Ag nanoparticle-modified gold electrode. Scan rate: 40 mV/s.

the electrode surface.

The electrochemical behaviors of BCB at bare gold electrode and the modified electrode were investigated. As shown in Figure 4b, when the bare gold electrode was placed into pH 7.0 PBS containing  $1.0 \times 10^{-5}$  mol/L BCB solution, a couple of ill-redox peaks were observed, which corresponds to the reduction and reoxidation of BCB. But the peaks did not appear at the BDT self-assembled monolayer modified gold electrode (Figure 4a). In contrast, in the same solution, the BCB showed a pair of a well-defined peaks at BDT self-assembled monolayer and Ag nanoparticle-modified gold electrode (as shown in Figure 4c), which cathodic and anodic potentials were  $-0.354$  and  $-0.299$  V (vs SCE), respectively. The formal potential<sup>16</sup> is  $-0.324$  V. The shapes of the cathodic and anodic peaks were nearly symmetric, and the cathodic reduction peak currents were almost equal to the anodic oxidation peak currents. Furthermore, the  $\Delta E_p$  was about 55 mV. The results indicated that Ag nanoparticles could promote the electron-transfer rate between BCB and electrode.

The dependence of peak currents ( $I_p$ ) and peak potentials ( $E_p$ ) on the scan rate ( $v$ ) was observed. The results indicated that  $I_p$  increased linearly with  $v^{1/2}$ , and the slope of  $\log(I_p)$  vs  $\log(v)$  was 0.96. On the other hand,  $E_p$  did not change when the scan rate increased. Herein, the redox process of BCB at the modified electrode was reversible.

The method was performed for determination of BCB by differential pulse voltammetry (DPV). The DPV peak currents increased linearly with concentration of BCB (Figure 5). A repetitive experiment was carried out with a solution of  $1.0 \times 10^{-5}$  mol/L BCB. The relative standard derivation (R.S.D) for eight repetitive measurements was 0.9%. The results indicated that the modified electrode displayed excellent reproducibility. After the experiments, the modified electrode was cleaned by water and stood in pH 7.0 PBS. The DPV currents of  $1.0 \times 10^{-5}$  mol/L BCB remained almost unchanged for two weeks and the currents only decreased to 98.7% after two weeks, which indicated that the modified electrode was very stable.

In conclusion, BDT can be self-assembled on the surface of gold electrode in a monolayer to form a BDT-modified electrode and Ag nanoparticles can be strongly adsorbed on the BDT-modified electrode to form a BDT self-assembled monolayer and Ag nanoparticle-modified electrode. The modified electrode has good electrocatalytic activity and can catalyze the redox-

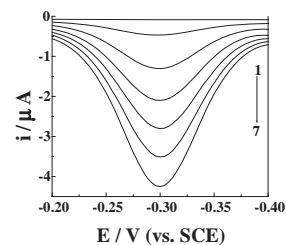


**Figure 5.** Differential pulse voltammograms of BCB at BDT self-assembled monolayer and Ag nanoparticle-modified gold electrode in PBS. The concentration of BCB (1–7):  $0$ ,  $1 \times 10^{-5}$ ,  $5 \times 10^{-5}$ ,  $9 \times 10^{-5}$ ,  $1.3 \times 10^{-4}$ ,  $1.7 \times 10^{-4}$ ,  $2.1 \times 10^{-4}$  mol/L. Pulse amplitude: 50 mV.

process of BCB. These results may help us to develop a new application in the field of electrocatalysis and amperometric detectors.

We thank the Science and Technology Foundation of Ministry of Education of China (No. 00117).

## References

- 1 G.-A. Ozin, *Adv. Mater.*, **4**, 612 (1992).
- 2 H. Kamaya, I. Ueda, and H. Eyring, "Molecular Mechanisms of Anesthesia. Progress in Anesthesiology," ed. by B.-R. Fink, Raven Press, New York (1980), Vol. 2, p 429.
- 3 T. Yoshida, H. Okabayashi, K. Takahashi, and I. Ueda, *Biochim. Biophys. Acta*, **722**, 1021 (1983).
- 4 S. Ribrioux, G. Kleymann, W. Haase, K. Heitmann, C. Ostermeier, and H. Michel, *J. Histochem. Cytochem.*, **44**, 207 (1996).
- 5 J.-F. Hainfeld and F.-R. Furuya, *J. Histochem. Cytochem.*, **40**, 177 (1992).
- 6 M.-D. Nada, M.-B. David, D.-J. Charles, T. Kenji, and R. Tijana, *J. Phys. Chem. B*, **105**, 954 (2001).
- 7 G. Sandmann, H. Dietz, and W. Plieth, *J. Electroanal. Chem.*, **491**, 78 (2000).
- 8 H.-Y. Gu, A.-M. Yu, and H.-Y. Chen, *J. Electroanal. Chem.*, **516**, 119 (2001).
- 9 X.-J. Han, W.-L. Cheng, Z.-L. Zhang, S.-J. Dong, and E.-K. Wang, *Biochim. Biophys. Acta*, **1556**, 273 (2002).
- 10 L. Wang and E.-K. Wang, *Electrochem. Commun.*, **6**, 49 (2004).
- 11 M. Ahav, A.-N. Shipway, I. Willner, M.-B. Nielsen, and J.-F. Stoddart, *J. Electroanal. Chem.*, **482**, 217 (2000).
- 12 M. Lahav, R. Gabai, A.-N. Shipway, and I. Willner, *Chem. Commun.*, **1999**, 1937.
- 13 W. Wang, S. Efrima, and O. Regev, *Langmuir*, **14**, 602 (1998).
- 14 B. Fang, Y.-C. Gao, M.-G. Li, and Y.-X. Li, *Mikrochim. Acta*, **147**, 83 (2004).
- 15 A.-B. Kharitonov, L. Alfonta, E. Katz, and I. Willner, *J. Electroanal. Chem.*, **487**, 133 (2000).
- 16 L. Zhang, G.-C. Zhao, X.-W. Wei, and Z.-S. Yang, *Chem. Lett.*, **33**, 86 (2004).
- 17 X.-H. Zhang, S.-F. Wang, and N.-J. Sun, *Bioelectrochemistry*, **65**, 41 (2004).